Mars Analysis Correction Data Assimilation: A Multi-Annual Reanalysis of Atmospheric Observations for the Red Planet

L. Montabone[1,2], S. R. Lewis[3], L. Steele[3], J. Holmes[3], P. L. Read[2], T. Ruan[2], M. D. Smith[4], D. Kass[5], A. Kleinböhl[5], J. T. Schofield[5], J. H. Shirley[5], D. J. McCleese[5]

[1]Université Pierre &Marie Curie, Laboratoire de Météorologie Dynamique, Paris, France
[2]University of Oxford, Department of Physics, AOPP, Oxford, UK
[3]The Open University, Department of Physical Sciences, UK
[4]NASA Goddard Space Flight Center, Greenbelt, MD, USA
[5]Jet Propulsion Laboratory, California Institute of Technology, Pasadena, CA, USA

British Atmospheric Data Centre
NATIONAL CENTRE FOR ATMOSPHERIC SCIENCE
NATURAL ENVIRONMENT RESEARCH COUNCIL

Available online at
http://badc.nerc.ac.uk/search
Contact e-mail: montabone@atm.ox.ac.uk

Mars Facts

Bulk and Orbital Parameters

- ✓ Mars Sidereal year ~ 1.88 x Earth (~ 687 days)
- ✓ Mars Mean solar day (sol) ~ 1.027 x Earth (~ 24h 40')
- ✓ Mars Eccentricity ~ 5.6 x Earth (= 0.0935)
- ✓ Mars Radius ~ 0.53 x Earth (~ 3396 km at Equator)
- ✓ Mars Gravity ~ 0.38 x Earth (~ 3.7 ms^{-2})

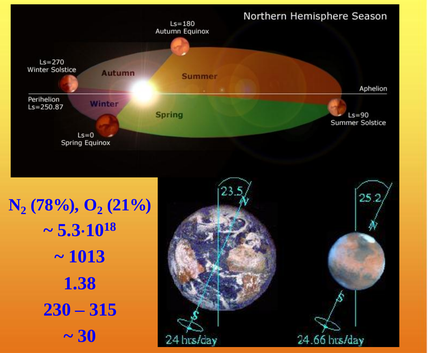

Atmospheric Parameters (Mars vs Earth)

✓ Composition:	CO_2 (95%), N_2 (2.7%)	N_2 (78%), O_2 (21%)
✓ Mass (kg) :	~ $2.5 \cdot 10^{16}$	~ $5.3 \cdot 10^{18}$
✓ Surface pressure (hPa) :	~ 6 (at mean radius)	~ 1013
✓ Solar constant (kW m^{-2}):	0.594	1.38
✓ Surface temperature (K):	140 – 290	230 – 315
✓ Radiative relaxation timescale (mean solar days)	1-2	~ 30
✓ Major absorber/scatterer of solar radiation (low atm.)	Dust	Water vapour

Outline

Ever increasing numbers of atmospheric observations from orbiting spacecraft, and increasingly sophisticated numerical atmospheric models, have recently permitted data assimilation techniques to be applied to planets beyond the Earth. Mars is the first extra-terrestrial planet for which reanalyses of the atmospheric state are now available [1,2,3].

We have reanalysed retrieved observations of temperature and dust optical depth from the Thermal Emission Spectrometer (TES [4]) on board NASA's Mars Global Surveyor (MGS) satellite and from the Mars Climate Sounder (MCS [5]) on board NASA's Mars Reconnaissance Orbiter (MRO) by assimilation into a Mars global circulation model (MGCM), making use of a sequential procedure known as the Analysis Correction scheme [6]. This is a form of successive corrections method which has proved accurate and robust under Martian conditions, even during the less-than-ideal MGS aerobraking period [7, 8]. The MGCM used at the University of Oxford and at The Open University consists of a spectral dynamical solver and a tracer transport scheme developed in the UK. Its package of state-of-the-art physical parameterization routines is shared with the LMD-MarsGCM, developed by the Laboratoire de Météorologie Dynamique in Paris (France) [9]. A typical reanalysis uses a T31 truncation and 25 or 32 vertical sigma levels. The reanalysis of retrieved TES water vapour and water ice optical depth, and MCS water ice optical depth is ongoing.

Overall, the application of our data assimilation scheme to retrieved observations from TES and MCS spans almost six complete Martian seasonal cycles. This represents a multi-annual climatology for Mars, which has the advantage of being a complete, dynamically-balanced, four-dimensional best-fit to observations for all the atmospheric variables, including those for which no direct measurements are available (e.g. wind and surface pressure) and with regions of no observations filled-in in a physically-consistent way.

Mars Reanalysis: Observations

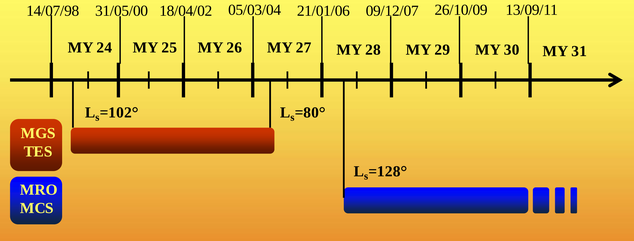

Mars years (MY) are labelled using the convention that MY 1 starts at northern hemisphere spring equinox of the year when the first scientific observation of a planet-encircling dust storm was carried out (1956). Within each year, the solar longitude (L_s) is used to represent the Martian "calendar". L_s is the angle between Mars, the Sun and the vernal point in Mars' orbit.

- ✓ Nadir thermal profiles (below ~40 km)
- ✓ Total (column) dust optical depth
- ✓ Total water vapour optical depth *
- ✓ Total water ice optical depth *

- ✓ Limb thermal profiles (below ~80 km)
- ✓ Limb dust optical depth profiles *
- ✓ Estimation of column dust optical depth
- ✓ Limb water ice optical depth profiles **

* Work in progress
** Future work

"Analysis Correction" Scheme

Gridpoint increments (horizontal analysis)

$$\Delta x_k = \lambda \sum_i \mu_{ki}\, Q_i R_i^2(\delta t_i) C_i$$

Observation locations
Time factor
Relaxation coefficient
Normalization factor

$$\mu_{ki} = \left(1 + \frac{r_{ki}}{S_i(\delta t_i)}\right) \exp\left(-\frac{r_{ki}}{S_i(\delta t_i)}\right)$$

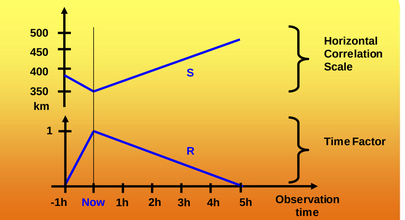

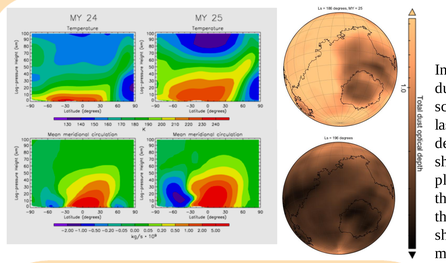

Atmospheric impacts of global dust storms

In MY 25 (as well as MY 28) a series of regional dust storms rapidly evolved attaining planetary scale and enshrouding Mars in a veil of dust that lasted for many sols (see maps of dust optical depth on the left). Dust is a strong absorber of short-wave radiation, and a high dust loading at planetary scale has profound impacts on the thermal structure of the atmosphere as well as on the circulation. The zonal mean plots on the left show the temperature structure and the mean meridional circulation on Mars around L_s=210° in a year with no global storm (MY 24) compared with MY 25 [10].

Teleconnection event during the MY 25 global dust storm

Maps of normalized total dust optical depth at 610 Pa show the evolution of the MY 25 global dust storm at three key times. The Hovmöller plot at 18° S latitude show the corresponding longitudinal displacements of the minima of the surface pressure anomalies (with respect to the trend average), likely linked to the displacement of surface wind patterns and the onset of new dust lifting centres. Only the diurnal component of the thermal tide (k=1, T=1, propagating westwards) and the non-migrating tide equivalent to a Kelvin wave (k=1, T=1, propagating eastwards) are included in the Hovmöller plot [11, 12].

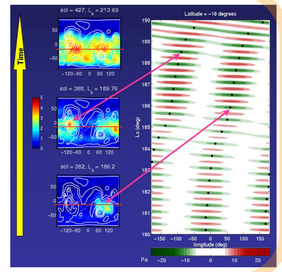

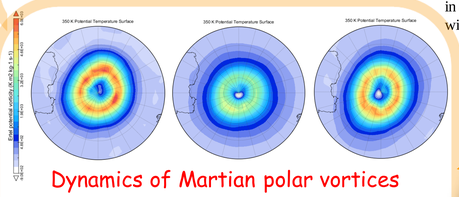

Dynamics of Martian polar vortices

During the winter seasons, Mars displays coherent polar vortices in both hemispheres, i. e. portions of its atmosphere at latitudes poleward of 60° are isolated by strong circumpolar jets in the altitude range 40-70 km. As in the Earth's stratosphere, Martian polar vortices play an important role in the transport of tracers and in the connection with the global circulation. The PV maps above (separated by 15 sols each and centred around L_s=324° in MY 26) show the impact of a regional dust storm occurring in the southern hemisphere on the northern polar vortex (another example of Martian teleconnection event).

Selection of results

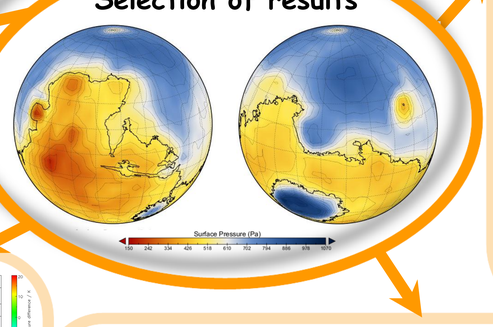

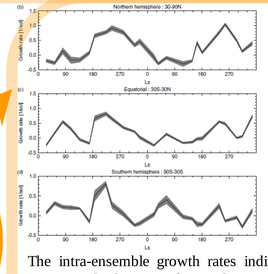

Predictability of Martian weather

A range of initial value forecasts were obtained and the growth rate of forecast errors measured against the reanalysis were determined as a function of season during MY 25 and 26 (Left Figure shows the mean daily growth rate at 30 Pa and its standard deviation).

The intra-ensemble growth rates indicate that internal baroclinic transients lead to significant chaotic growth of model 'error' on time-scales of 3–10 sols only during northern hemisphere autumn and winter seasons. At other seasons, ensembles retain coherence at least over several tens of sols. Imperfections in dust distribution and coupling with other aerosols can lead to large errors in the dust field when it evolves rapidly, and rapid divergence of the entire ensemble from the observed atmospheric state. Predictability on Mars is very challenging despite the fact Mars' atmosphere seems less complex and chaotic than its terrestrial counterpart [13].

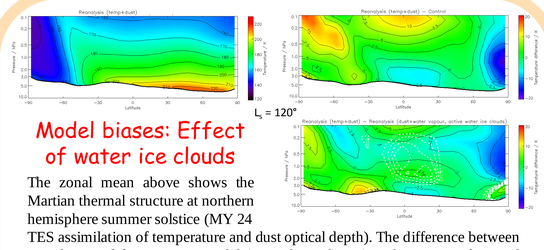

Model biases: Effect of water ice clouds

The zonal mean above shows the Martian thermal structure at northern hemisphere summer solstice (MY 24 TES assimilation of temperature and dust optical depth). The difference between reanalysis and free running model (control simulation) in the upper right panel highlights biases in the MGCM. In particular, the model cold equatorial bias above 1 hPa is associated with the lack of water ice cloud modelling in the control simulation run. When the temperature+dust reanalysis is compared to a reanalysis of only dust+water vapour and water ice clouds modelling is introduced in the MGCM allowing for radiative effects, the equatorial bias disappears (lower right panel. Dashed contours represent water ice clouds). [14]

Solsticial pause in baroclinic wave activity

Baroclinic (transient) waves are prominent at high latitudes in the winter Martian seasons, although the eccentricity of the orbit of the planet makes the northern hemisphere winter waves have much larger amplitude. The signal of the baroclinic waves can be clearly seen, for instance, in the temperature, meridional wind (upper right panel) and surface pressure (lower right panel). What can also be clearly noticed is the "pause" in the wave activity that occurs around winter solstice (L_s~270° in the northern hemisphere) [15]. Recent free running MGCM simulations have verified that radiatively active clouds alter the thermal structure of the atmosphere and decrease the vertical shear of the westerly jet near the surface around solstice, shifting the lower portion of the jet equatorwards [16].

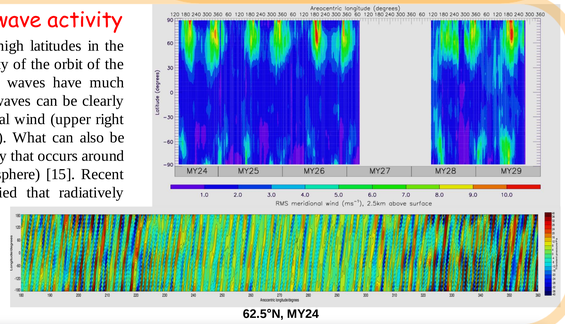

References

[1] Montabone, L., et al., NCAS British Atmospheric Data Centre, http://badc.nerc.ac.uk, 2011 [2] Greybush, S. et al., JGR Planets, 2012, submitted [3] Lee, C. et al., JGR Planets 116, E15, 2011 [4] Christensen, P.R. et al., J. Geophys. Res. 106, 2001 [5] McCleese, D.J. et al., J. Geophys. Res. 112, 2007 [6] Lorenc, A.C. et al., QJRMS 117, 1991 [7] Lewis, S.R. et al., Icarus 192, 2007 [8] Montabone, L. et al., Icarus 185, 2006 [9] Forget, F. et al., 3rd MAMO, Williamsburg, VA, USA, N. 1447, 2008 [10] Montabone, L. et al., Adv. Space Res. 36, 2005 [11] Montabone, L. et al., 3rd MAMO, Williamsburg, VA, USA, N. 1447, 2008 [12] Martinez-Alvarado, O. et al., Ann. Geophys. 29, 2009 [13] Rogberg, P. et al., QJRMS 136, 2010 [14] Wilson, R.J. et al., GRL 35, 2008 [15] Lewis, S.R. et al., in preparation [16] Mulholland, D. et al., 2012, in preparation